



SBIR- 08.10-9000
Release Date 6/27/92 ✓

FINAL REPORT

Contract Number: NAS7-1034

SBIR Phase II Program

7N-36
135816
P-43

1.083 Micron Tunable CW Semiconductor Laser

submitted by:

N93-16689

Unclas

G3/36 0135816

General Optronics Corp.

2 Olsen Ave., Edison, NJ 08820

to

NASA Resident Office

JET Propulsion Laboratory

4800 Oak Grove Drive

Pasadena, California 91109

June 28, 1991

(NASA-CR-191338) THE 1.083 MICRON
TUNABLE CW SEMICONDUCTOR LASER
Final Report (General Optronics
Corp.) 43 p

Final Report

Contract Number: NAS7-1034

1.083 Micron Tunable CW Semiconductor Laser

Table of Contents

1.	Objective of the Program.....	1
2.	Summary.....	2
3.	Introduction.....	3
4.	Device structure and Fabrication Procedures.....	4
	4.1 Device Structure and Crystal Growth.....	4
	4.2 Device Fabrication.....	8
5.	Device Characteristics.....	12
6.	Development of a Hermetically Sealed Package.....	15
7.	Temperature and Power Stabilization.....	19
8.	Temperature and Current Tuning of Laser Diode to He lines	27
9.	Life-Test.....	33
10.	Delivery of Prototype Units.....	34
11.	Conclusions.....	38
12.	References.....	39

Figure Captions

- Figure 1 Structure of Single Longitudinal Mode 1080 nm ----- 5
Laser Diode
- Figure 2 Liquid Atomic Fractions as a Function of Solid ----- 6
Composition for LPE Growth of $\text{Ga}_x\text{In}_{1-x}\text{As}_y\text{P}_{1-y}$
Lattice Matched to [100] InP at 635°C.
- Figure 3 SEM Photograph of CNS Laser Structure ----- 8
- Figure 4 L/I and V/I curve of a 1083 nm Laser Diode ----- 11
- Figure 5 Spectrum of a 1.083 Micron Laser Diode ----- 12
- Figure 6 Far Field of the Light Output from a 1083 nm ----- 13
Laser Diode
- Figure 7 Temperature Dependence of L/I curves for a 1083 --- 15
nm Laser
- Figure 8 Spectrum of 1083 nm Laser that can be stabilized -- 16
at He Absorption Lines
- Figure 9 Coherent Length measurement of a 1083 nm Single --- 17
Mode Laser
- Figure 10 Oxygen Free Copper Heat Sink For 1083 nm ----- 19
Laser Diode
- Figure 11 Hermetically Sealed TO-8 Package ----- 20
- Figure 12 Circuit Diagram of a Laser in TO-8 Package ----- 21
- Figure 13 Circuit Diagram for Power and Temperature ----- 24
Stabilization of a Laser Diode
- Figure 14 Housing for Two Stage Temperature Controlled ----- 25
Laser
- Figure 15 Temperature Stability of a Two Stage thermo ----- 26
-electric cooler controlled Laser Package
- Figure 16 Energy Diagrams of HeII Absorption Lines ----- 29
- Figure 17 Diagram of He Cell and RF source ----- 30
- Figure 18 Temperature and Current Tuning Characteristics --- 31
of Laser 1.083-10 for He Absorption Lines
- Figure 19 Temperature and Current Tuning Characteristics --- 32
of Laser 1.083-15 for He Absorption Lines

Figure 20	Life-Test Data of 1083 nm Laser Diodes -----	34
Figure 21	Temperature and Current Tuning Characteristics --- of Laser 1.083-19 for He Absorption Lines	36
Figure 22	Temperature and Current Tuning Characteristics --- of Laser 1.083-23 for He Absorption Lines	37

1. Objective of the Program

This program was initiated in response to NASA 86-1 SBIR solicitation subtopic 08.10. The statement of work from the solicitation is as follows:

08.10 Subtopic: Tunable CW Laser for the 1.08 Micron Region

A tunable CW laser is desired to produce light equivalent to the helium spectral line at 1.08 microns. This laser will serve as an optical pumping source for He3 and He4 atoms used in space magnetometers. This light source can be fabricated either as a semiconductor laser diode or a pumped solid state laser. Continuous output power of greater than 10 mW is desired. Semiconductor lasers can be thermally tuned, but must be capable of locking onto the helium resonance lines. Solid state lasers must have efficient pumping sources suitable for space configuration. Additional requirements: space magnetometer applications will include low mass (<0.5 kg.), low power consumption (<0.75 W), and high stability/ reliability for long missions (5-10 years).

2. Summary

Continuous wave operation of a 1.08 micron InGaAsP/ InP double heterostructure semiconductor laser has been successfully achieved utilizing a channelled substrate narrow stripe (CNS) structure. The fabrication process utilizes one-step liquid phase epitaxy. The project goals of 10 mW continuous output power and 1.083 micron emission wavelength have been achieved. The lasers have a typical threshold current around 80 mA and over 10 mW output power at an operating temperature of 20 degree C. The emission wavelength is tunable with wide temperature and current ranges to match the HeII absorption lines $D_0(10829.08 \text{ \AA})$, $D_1(10830.25 \text{ \AA})$ and $D_2(10830.34 \text{ \AA})$. A temperature and power stabilization electronics circuit has also been design to control the output power and temperature of the laser to within 0.02°C . This temperature control is required for the lasing wavelength to stay within the Doppler width of the absorption lines. Temperature stability of within 0.005°C has been demonstrated over a few weeks period. Operation life-test of the lasers has also been performed at 30°C . No failure or degradation has been observed over 3000 hours of life-test. Four operating units, which can be tuned to all the absorption lines, have been delivered to JPL Magnetometer Laboratory.

3. Introduction

A Vector Helium Magnetometer (VHM) developed by Jet Propulsion Laboratory in the mid 1970's [1] has impressive sensitivity of 0.01 nT (10^{-7} gauss)[2]. Many such VHM's have since been utilized successfully in various space missions. The VHM enables scientists to accurately measure the interplanetary magnetic fields and the detailed structure of the magnetosphere of various planets. An RF powered helium discharge tube is used as the light source for pumping the helium magnetometer. Recent advances in semiconductor lasers offer an opportunity to further improve the sensitivity and miniaturize the Vector Helium Magnetometer. The use of a semiconductor laser for pumping such helium magnetometers is particularly advantageous because of their small size, low voltage operation, low power consumption and high reliability.

It is well known that because the composition of the quaternary active layer of an InGaAsP/InP laser can be adjusted, The lasing wavelength of the laser can range from 1 micron to 1.7 micron. However, for wavelength shorter than $1.1 \mu\text{m}$ Continuous Wave (CW) room temperature operation become much more difficult, because the potential and refractive index differences between cladding layer and the active layer are small.

In this report we describe the development of the quaternary $1.083 \mu\text{m}$ wavelength InGaAsP/InP laser which has achieved results better than the original goals.

4. Device Structure and Fabrication Procedures

4.1 Device Structure and Crystal Growth

The structure of a quaternary InGaAsP/InP CNS laser is shown schematically in Figure 1. The CNS laser has been grown using a one-step liquid phase epitaxy (LPE). Before LPE growth, Cd diffusion is performed on the n-type InP substrate to facilitate a reverse junction for eliminating leakage current outside the channels. Cd instead of Zn is used because Cd has been shown to diffuse much more slowly and does not further diffuse into the LPE layers during the crystal growth. The Cd diffusion is performed at 600 degree C using a mixture of InP powder, Cd_3P_4 and red phosphorus as the source. It requires 12 minutes to obtain $0.5 \mu m$ diffusion depth. The use of phosphorus provides sufficient vapor pressure to prevent InP surface decomposition. Channels with $4.5 \mu m$ width and $1.5 \mu m$ depth were etched through the diffusion layer before the LPE growth. The chemical etchant used is a BPK solution ($2HBr : 4H_3PO_4 : 1N K_2Cr_2O_7$) and the etching time is 30 seconds at 5 degree C.

By using the phase diagram of $Ga_xIn_{1-x}As_yP_{1-y}$ and the conditions for lattice matching to InP, melt compositions can be obtained properly for growing an active layer having an emission wavelength between 1 micron and 1.7 micron. Use of the phase diagram as shown in Figure 2 together with an equation relating the band-gap energy $E_g(y)$ and the composition:

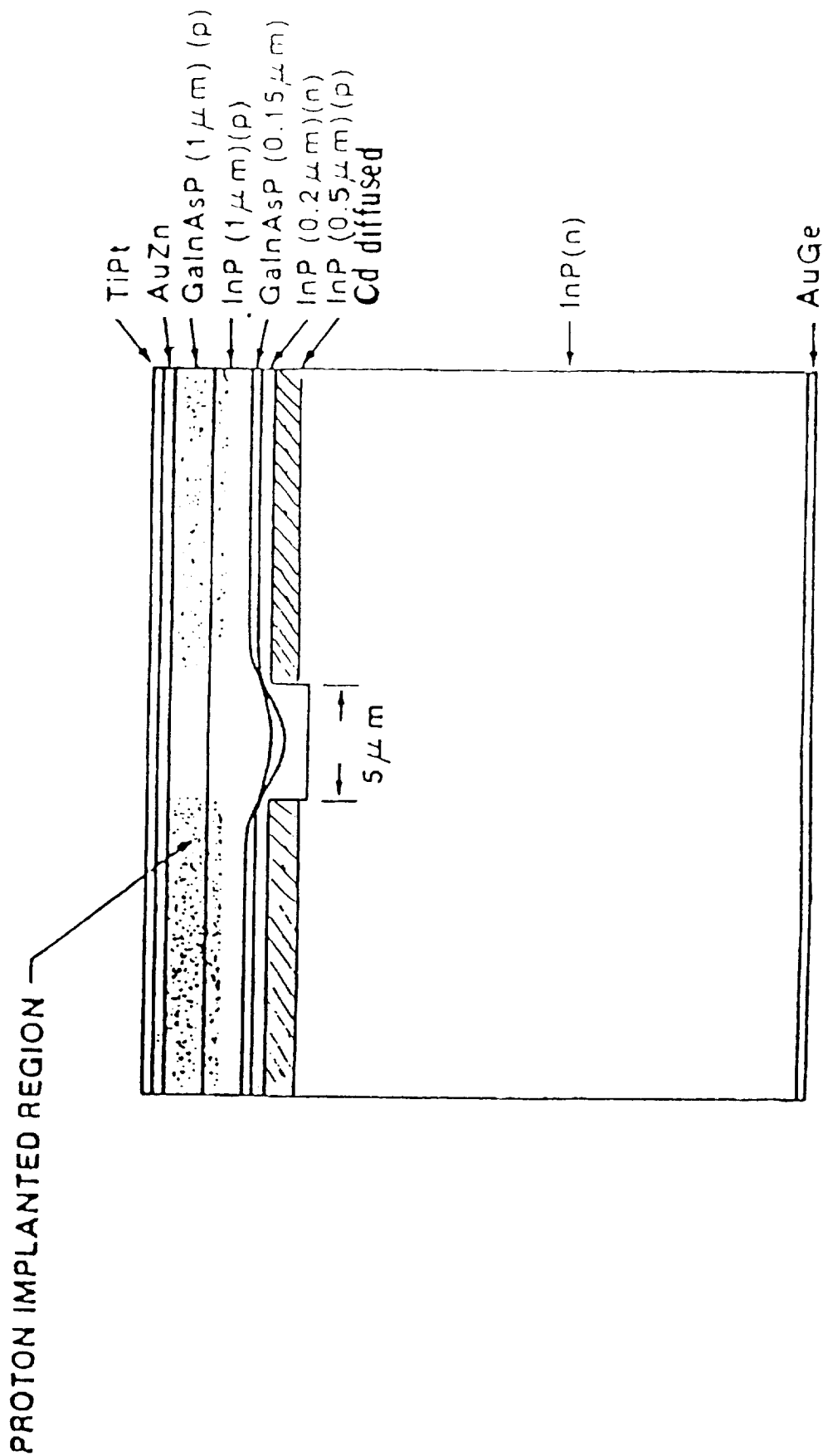


Figure 1.

STRUCTURE OF SINGLE LONGITUDINAL MODE LASER DIODE AT $1,080\text{nm}$
 (CHANNELLED SUBSTRATE NARROW STRIPE LASER)

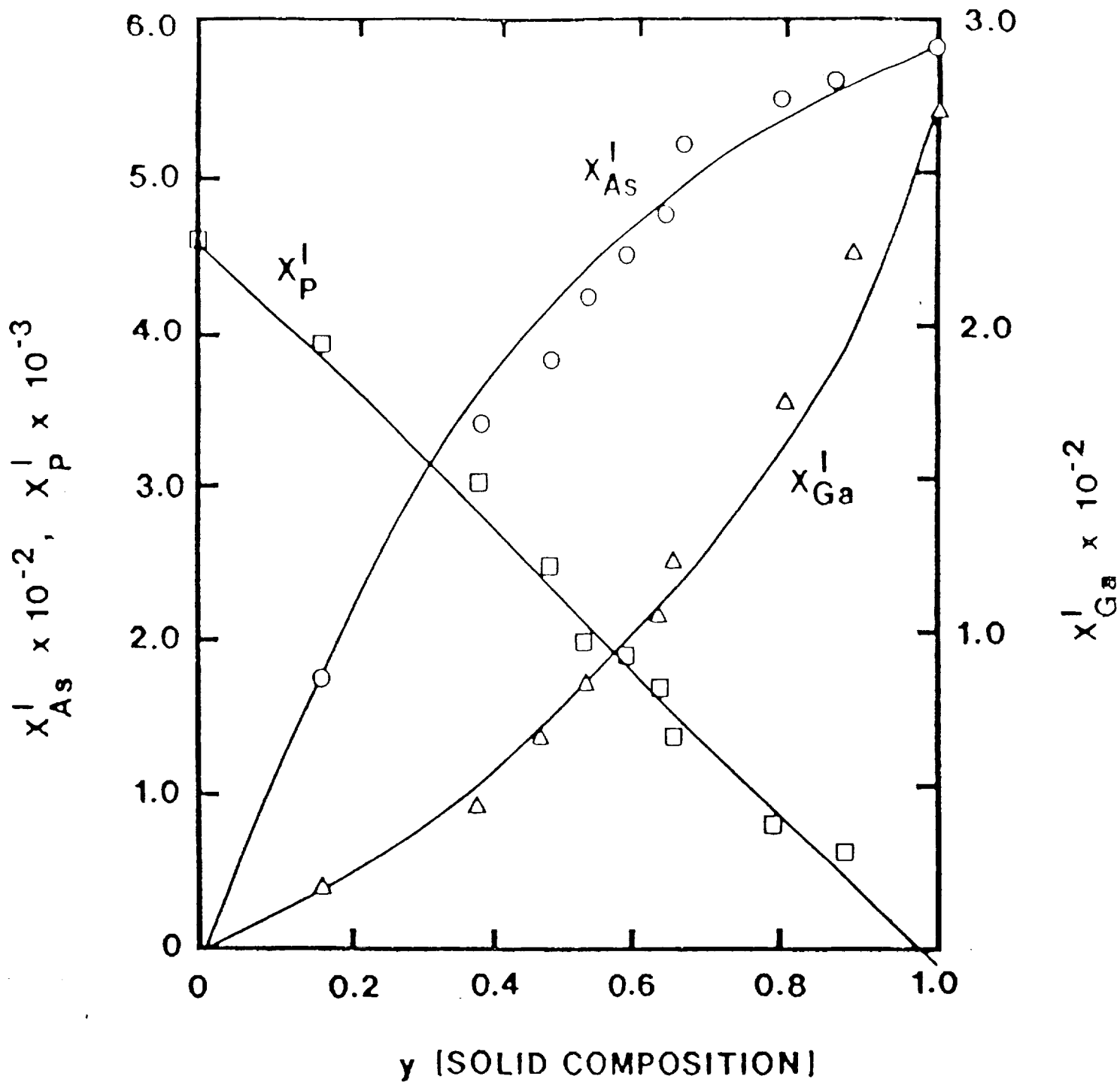


Figure 2. LIQUID ATOMIC FRACTIONS X_{As}^I , X_P^I , X_{Ga}^I AS A FUNCTION OF SOLID COMPOSITION y , FOR LPE GROWTH OF $Ga_x In_{1-x} As_y P_{1-y}$ LATTICE MATCHED TO [100] InP AT 635°C.

$$E_g(y) = 1.35 - 0.72 y + 0.12 y^2 \quad (\text{eV})$$

enabled us to find the fractions of As, P and Ga in the Indium solution for proper growth of the quaternary compound having an emission wavelength at 1.08 μm . The corresponding solid composition is obtained from the above equation and Vegard's Law for $\text{Ga}_x\text{In}_{1-x}\text{As}_y\text{P}_{1-y}$ lattice matched to InP which is given by:

$$a(x,y) = 0.1894y - 0.4184x + 0.013xy + 5.8696$$

where $a(x,y) = a(\text{InP}) = 5.8696 \text{ \AA}$.

Thus, the solid composition for the 1.083 μm active layer is $\text{Ga}_{0.16}\text{In}_{0.84}\text{As}_{0.35}\text{P}_{0.65}$.

Before placing the substrate into the crystal growth furnace, the substrate was cleaned with Acetone, Methanol and TCE. Also, it was etched with $5\text{H}_2\text{SO}_4 : 1 \text{H}_2\text{O}_2 : 1 \text{H}_2\text{O}$ solution for one minute. The melts are baked in the Indium solution for one hour each at high (656 degree C) and Low (646 degree C) temperature. The temperature is then decreased with a small ramp at a cooling rate of 0.4 degree C/min. Crystal growth starts at 635 degree C. Four LPE layers are grown which consist of: 0.2 μm Sn doped InP buffer layer (1 min), 0.15 μm undoped InGaAsP active layer (10 sec), 1.0 μm Zn doped InP confinement layer (10 min) and 1.0 μm Zn doped InGaAsP contact layer (5 min). Figure 3 shows the scanning electron microscope photograph of the cross section of this laser.

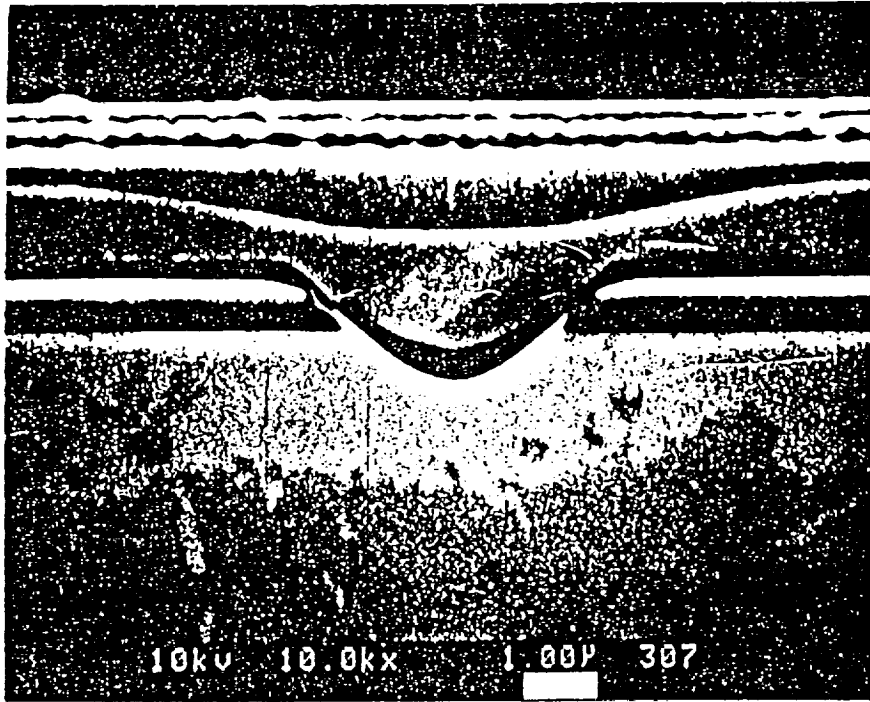


Figure 3. SEM Photograph of CNS Laser

4.2 Device Fabrication

After the wafer is grown, the wafer is first processed with p-contact. This is done in three sequential steps: Zn skin diffusion, AuZn metal deposition and Ti-Pt thin layer sputtering. The wafer is then lapped in the n side to a thickness of between 75 and 100 μm . The N-contact is applied by evaporation of AuGe alloy. Both P and N contacts are then alloyed at 410 degree C. to form a good ohmic contact. Electroplated gold stripes 4 to 5 μm wide and 3 μm height are formed on the P surface to serve as masks for proton implantation. The implantation voltage is adjusted according to the thickness of the top two LPE layers. Since the performance of such InGaAsP/InP lasers are more sensitive to temperature, efficient heat extraction is important. Hence, a gold-plated heat sink of 12 μm thick is applied to each laser chip to help spread the heat into a larger heat sink. The wafer is cleaved into chips of the size 250 μm X 250 μm . The chips are then mounted P-side down on the heat sink.

5. Device Characteristics

Under phase I program, continuous wave operation of a 1.08 micron InGaAsP/ InP double hetrostructure semiconductor laser has been successfully achieved.

The threshold current for most of the devices is between 75 mA and 90 mA at 10 degree C. The output power exceeded 10 mW with 200 mA of driving current. A typical light output power versus drive current curve at 10 degree C is shown in Figure 4. As the temperature is increased to 20 degree C., the threshold current increases to 100 mA and the maximum output power drops to 4 mW.

The peak wavelength of the lasers that have been tested is in the range of 1.081 micron to 1.084 micron. Figure 5 shows the spectra distribution of the laser which was measured at 5 mW output power and 10 degree C temperature. The wavelength can be changed continuously with different drive currents and temperatures.

The far field patterns for directions parallel and perpendicular to the junction plan are shown in Figure 6. The far-field patterns are measured at 110 mA drive current with output power of 5 mW at 10 degree C ambient temperature. The curve shows very good fundamental transverse mode operation. The angles of half intensity for parallel and perpendicular directions are 22 degrees and 38 degrees respectively.

GENERAL OPTRONICS CORP.
2 Olsen Avenue
Edison, NJ 08820

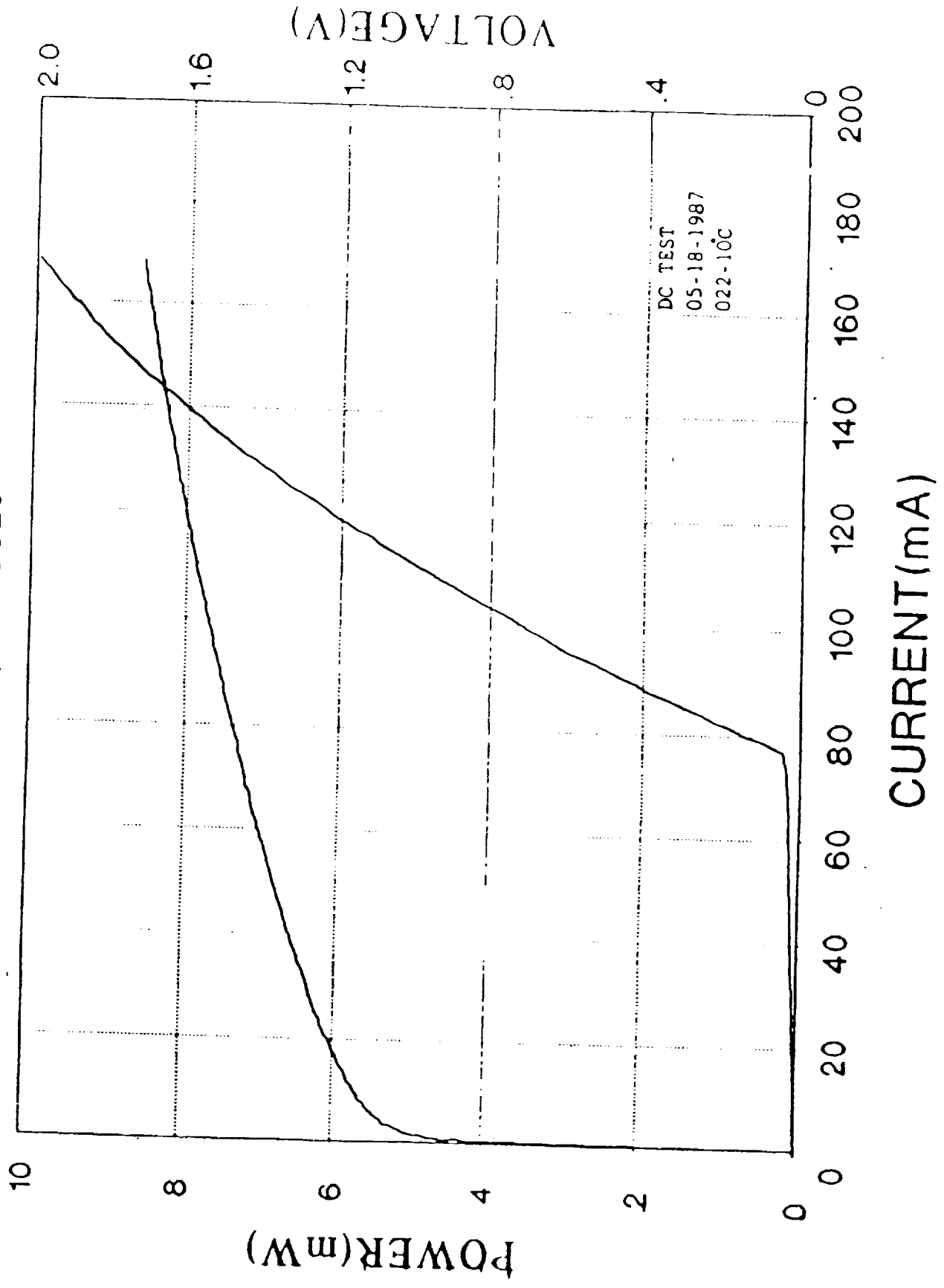


Figure 4. Light output power (L) and voltage (V) versus drive current (I) of a 1.08 um laser diode

Laser: 022-10C
Power: 5 mW

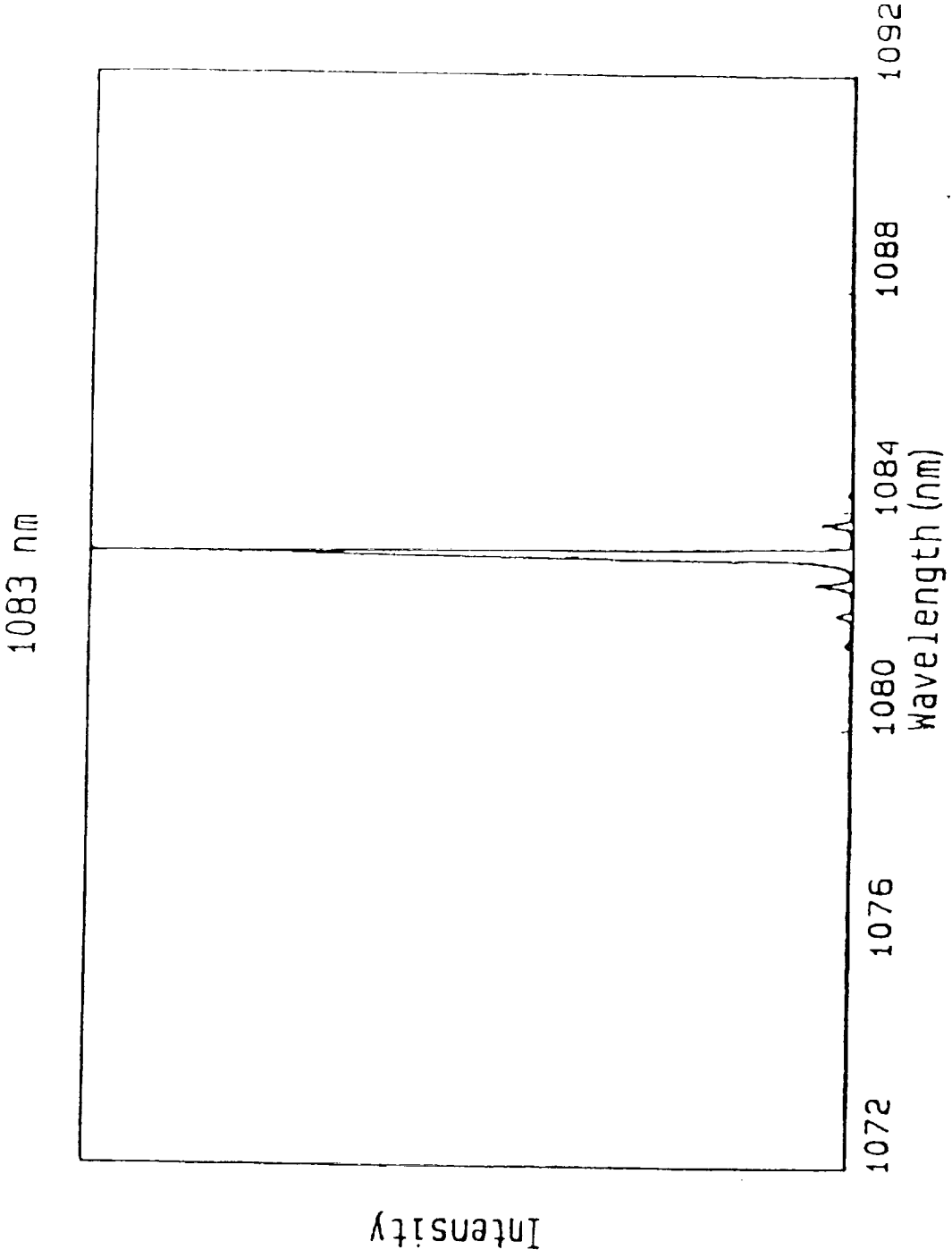


Figure 5. Spectrum of a 1.083 micron laser diode

GENERAL OPTRONICS CORPORATION
2 OLSEN AVE. EDISON, NJ 08820

LASER / ~~LED~~ # 022-100
CURRENT 110 mA
POWER 5 mW

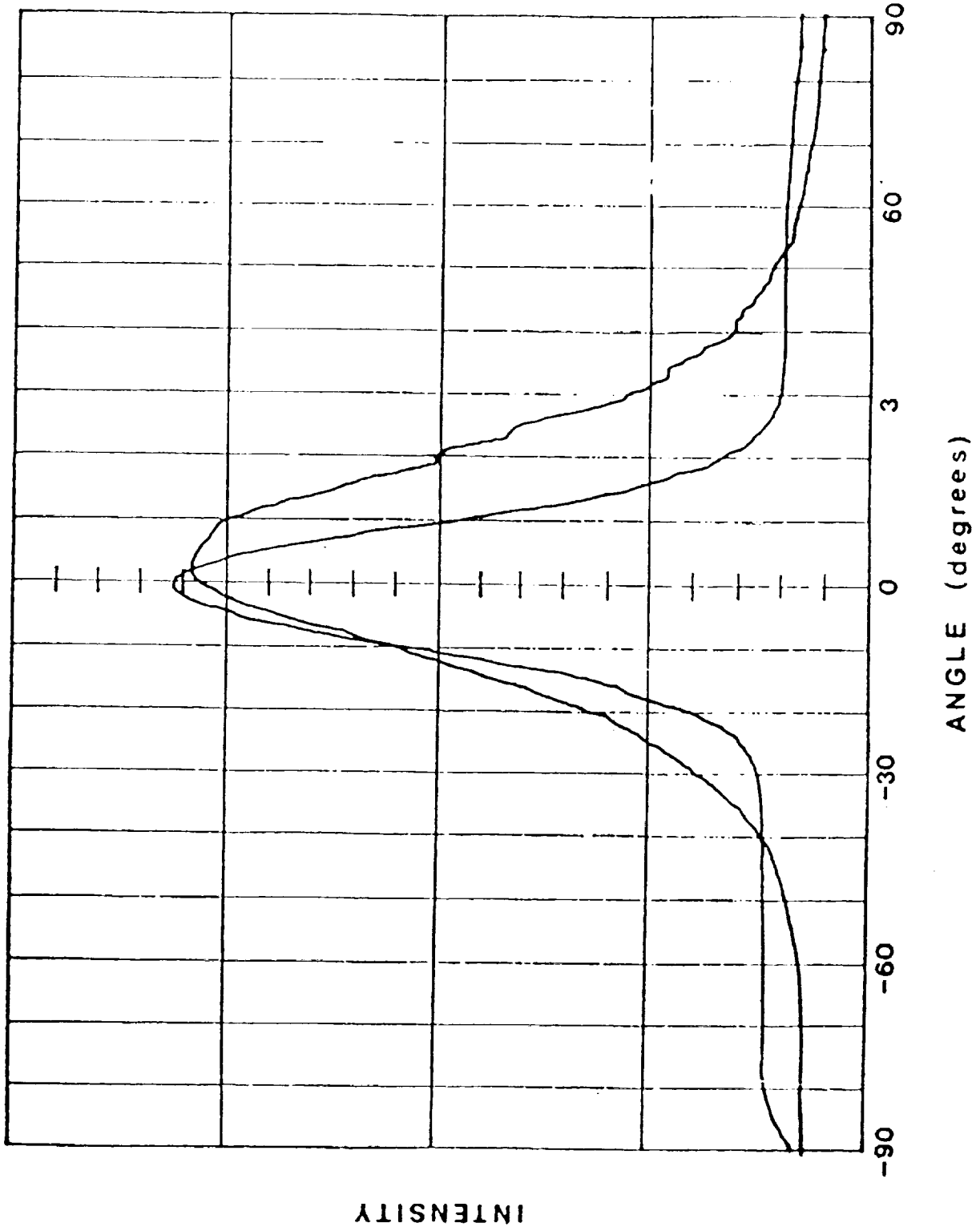


Figure 6. Far field of the light output from a 1.083 um laser diode

In phase II we have performed the optimization by adjusting the compositions and growth temperature to obtain good lattice matching and strong photoluminescent intensity. The resulting laser can operate at a higher temperature with better characteristics. 10 mW output power at 30°C operation can be obtained. Figure 7 shows the temperature dependence of the light versus current curve of a 1.083 μm laser. The characteristic temperature T_0 is about 40 degrees K. Figure 8 shows a typical spectrum, the side mode suppressing has improved significantly. A coherent length measurement as shown in figure 9 indicate that the coherent length is longer than 30 cm. This means that the line width is less than one GHz or the Doppler width of the absorption lines.

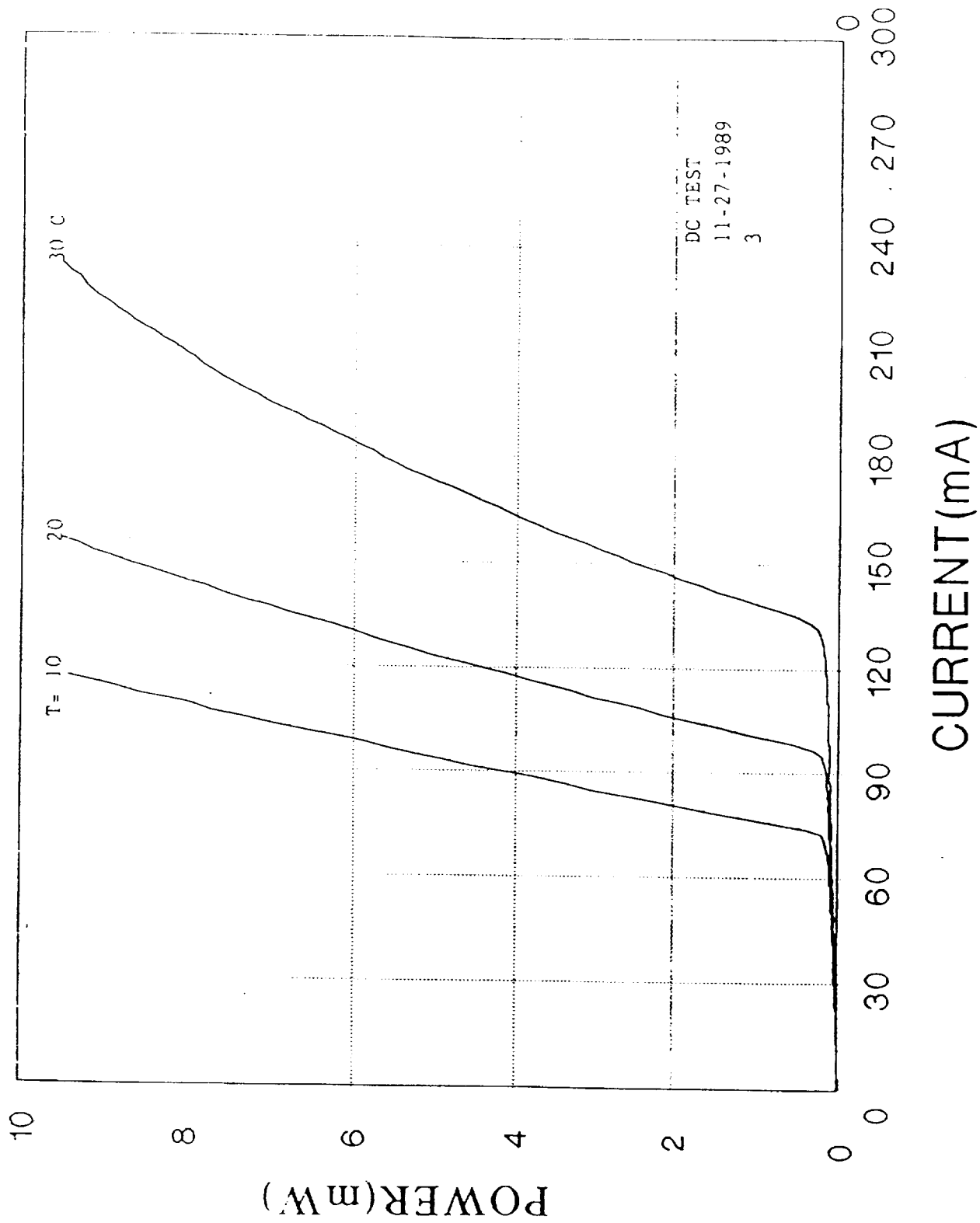
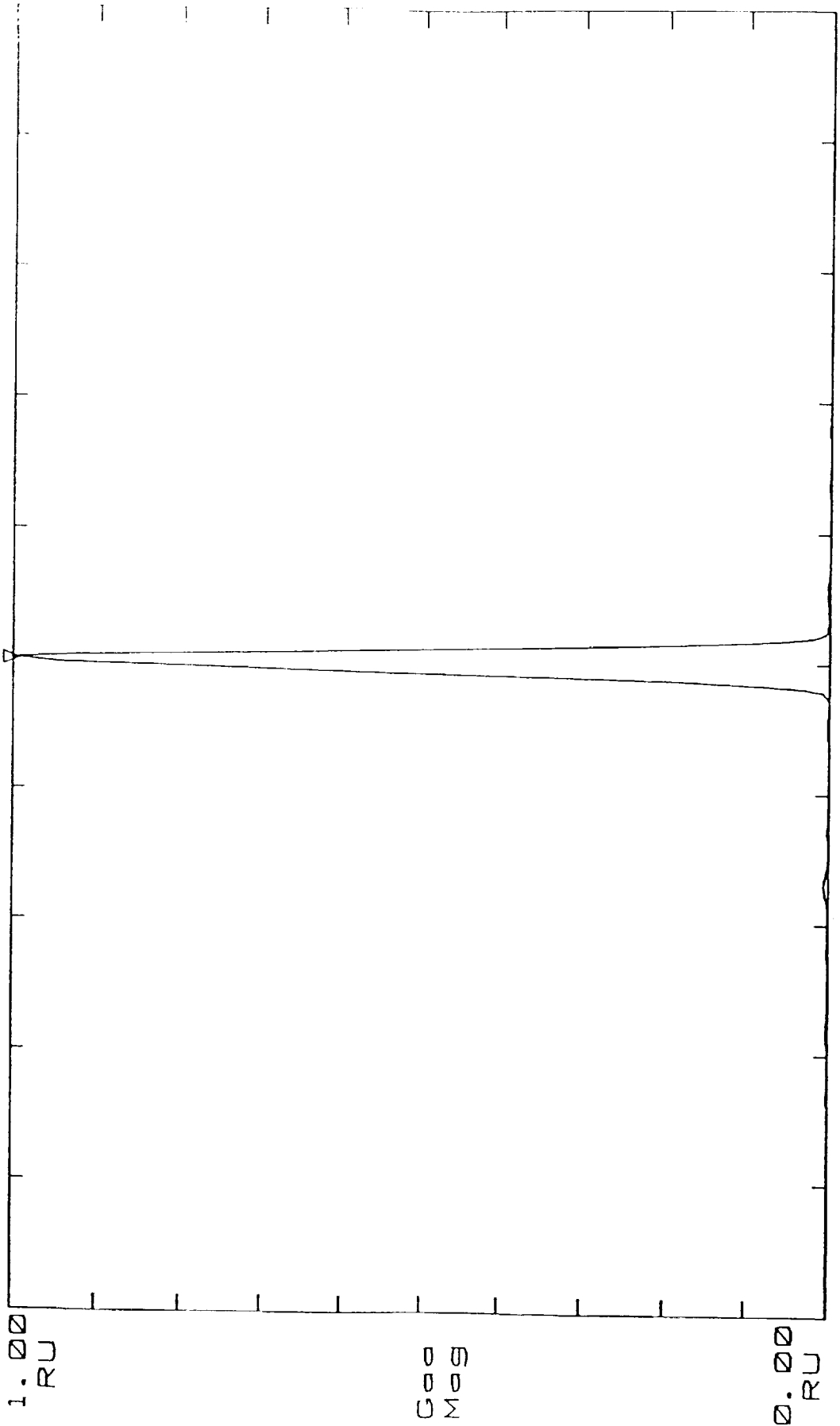


Figure 7 Temperature Dependence of L/I curves for a 1083 nm Laser

1.083-4
 09-09-1988 12:33 AVG 0/0 SPECTRUM
 PK . 1.083 02 μm 1.00E+00 RU



START STOP
 1.078 0 μm <1.083 01 μm > 1.088 0 μm
 λ_0 : 1.08300 μm $\Delta\lambda$: 0.16 μm PK NO. :

Figure 8 Spectrum of 1083 nm Laser that can be stabilized at He Absorption Lines

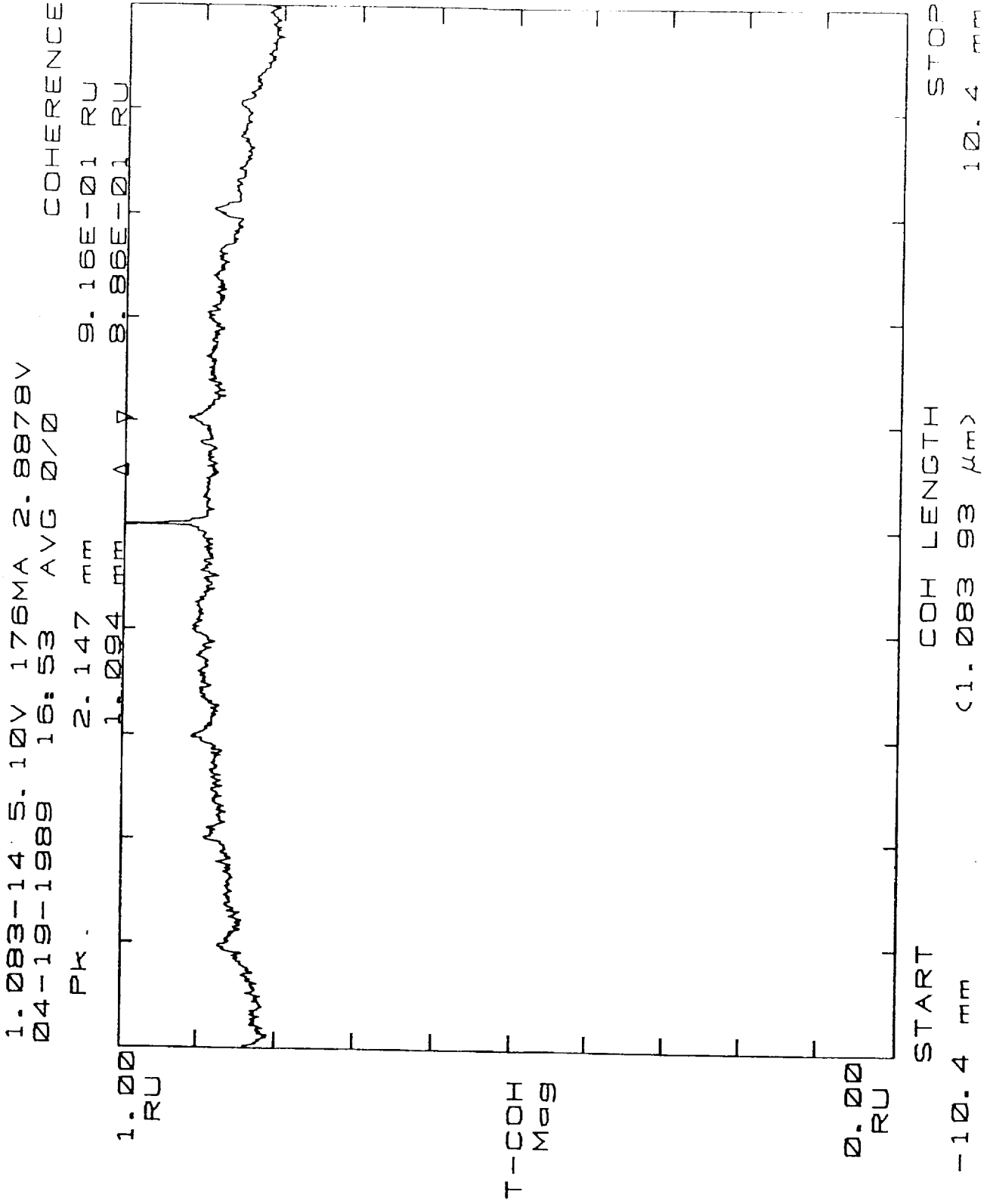


Figure 9 Coherent Length measurement of a 1083 nm Single Mode Laser

6. Development of a Hermetically Sealed Package

The lasers are mounted on standard General Optronics' heat sinks as shown in Figure 10. These heat sinks are made of oxygen free copper. Next to diamond, oxygen free copper has the highest thermal conductivity. With evaporated indium for die bonding, we can obtain very low thermal resistance of 25 degrees C per watt which gives good laser reliability.

A hermetically sealed TO-8 package as shown in Figure 11 are used for housing the laser. A detector, a thermistor and a thermal electric cooler are also installed in the package for feedback stabilization of the temperature and optical power. The pin assignments as well as dimensions are also shown in the figure. The equivalent circuit for the TO-8 laser package is shown in Figure 12. The laser in this package can be directly modulated up to 2 GHz.

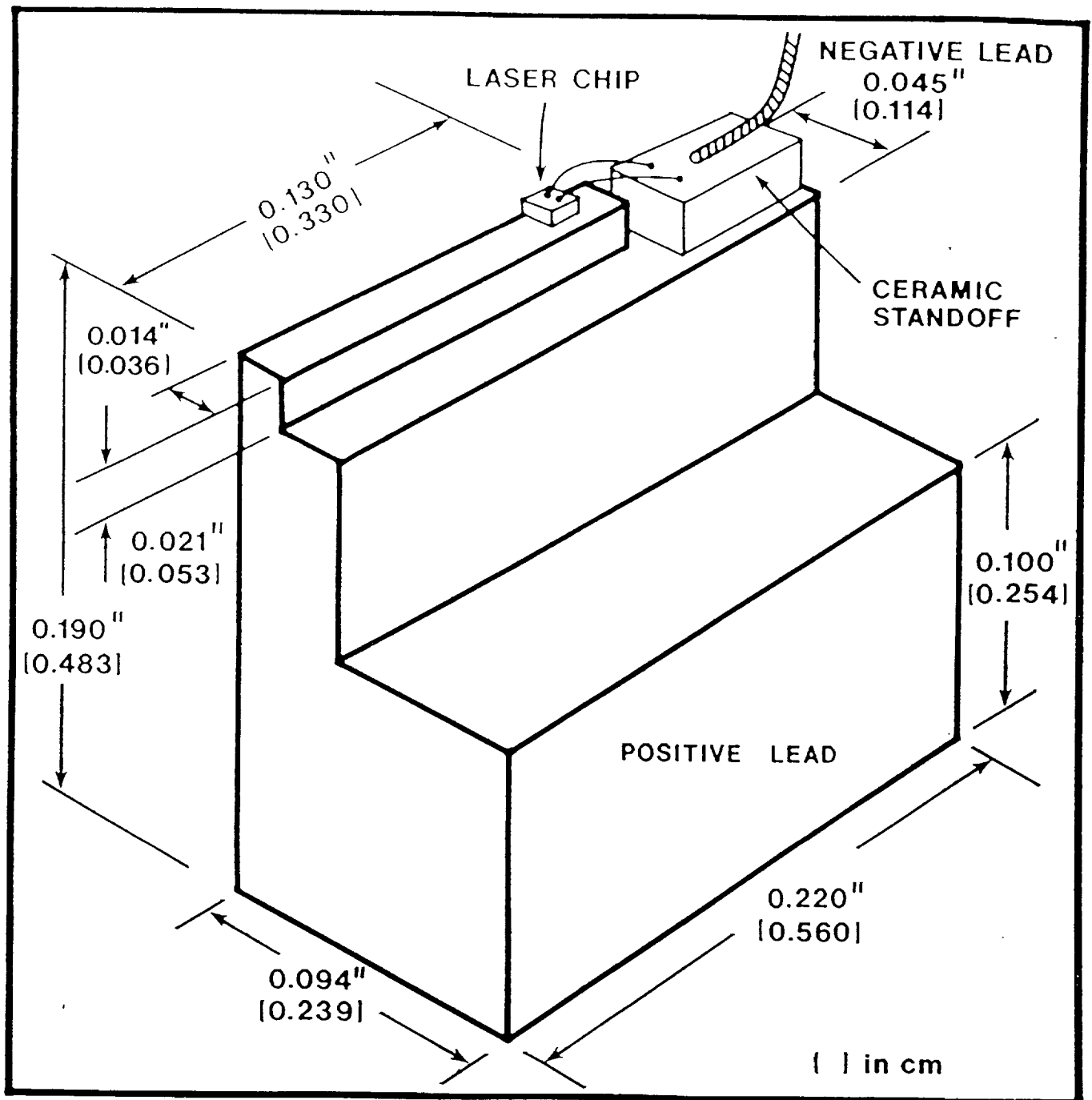
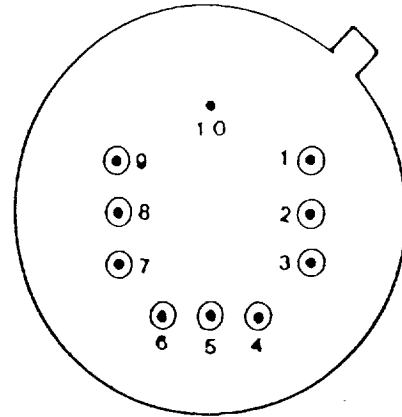
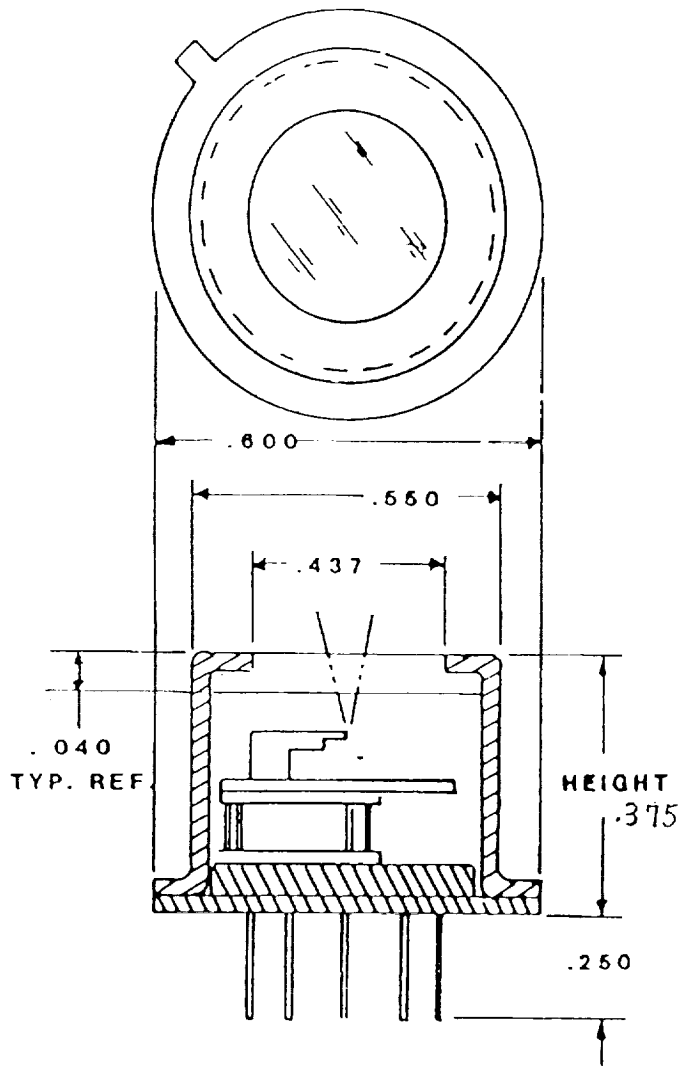


Figure 10 Oxygen Free Copper Heat Sink For 1083 nm Laser Diode



PIN CONFIGURATION	
1	COOLER (+)
2	THERMISTOR
3	DC BIAS INPUT
4	PHOTODETECTOR CATHODE
5	PHOTODETECTOR ANODE
6	LASER ANODE
7	LASER CATHODE
8	COOLER (-)
9	RF INPUT
10	Ground

Figure 11 Hermetically Sealed TO-8 Package

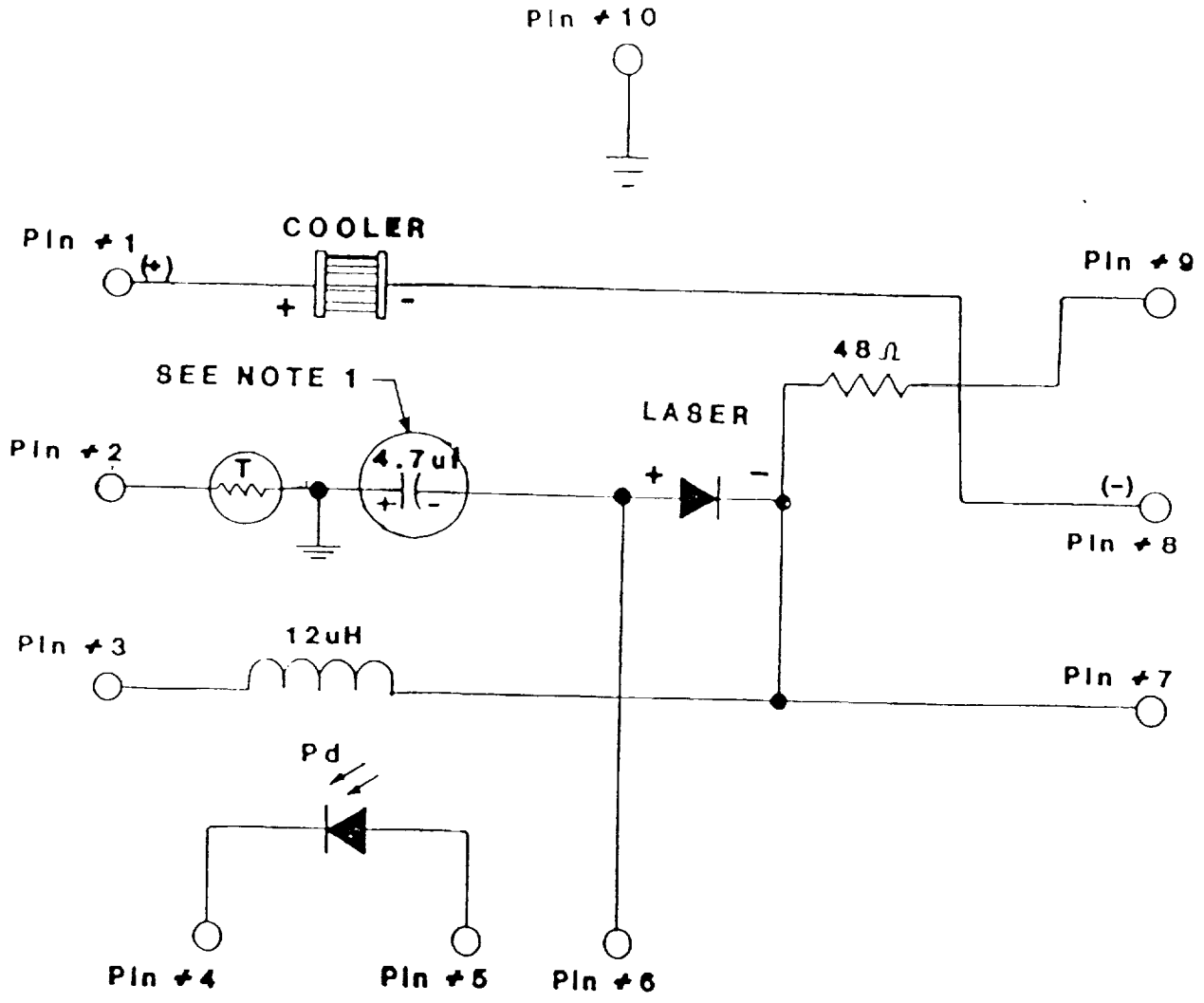


Figure 12 Circuit diagram of a Laser in TO-8 Package

7. Temperature and Power Stabilization

The lasing wavelength of the semiconductor laser can change substantially with changing output power or heat sink temperature. The wavelength change as a function of temperature is typically 1 Angstrom/degree C. Therefore, in order to operate at helium absorption wavelength of 1.083 microns the heat sink temperature and the optical power should be stabilized. With the attached detector in the backside of the laser and with a thermal electric cooler and a thermistor, electronic circuits can be designed to stabilize the temperature to within 0.02 degrees C and output power to within 1%. The electronic diagram of the temperature and power control circuit is shown in figure 13. With this circuit the temperature of the laser can be stabilized to 0.01°C in the range of -15°C to 30°C, the laser current can be from 0 to 250 mA. If higher current is required the power transistor Q_1 should be replaced with another transistor with higher current rating.

A two stage temperature control system has been build to test how well we can control the laser temperature. Figure 14 shows the housing of the two stages temperature controlled 1083 nm laser diode. IXL model LDM-4412 laser diode mount was utilized. Figure 15 shows the data taken for two stages temperature controlled system. Figure 15a shows the variation of room temperature which spans 3.1°C over a period of 4000 minutes. With one stage thermo-electric cooler control the laser plate temperature variation (Figure 15b) is within 0.0116°C during the same period. The laser, Which sit on this plate has another thermo-electric cooler for temperature

stabilization. The variation of laser temperature (Figure 15c) was less than 4.12×10^{-3} degrees C over 4000 minutes.

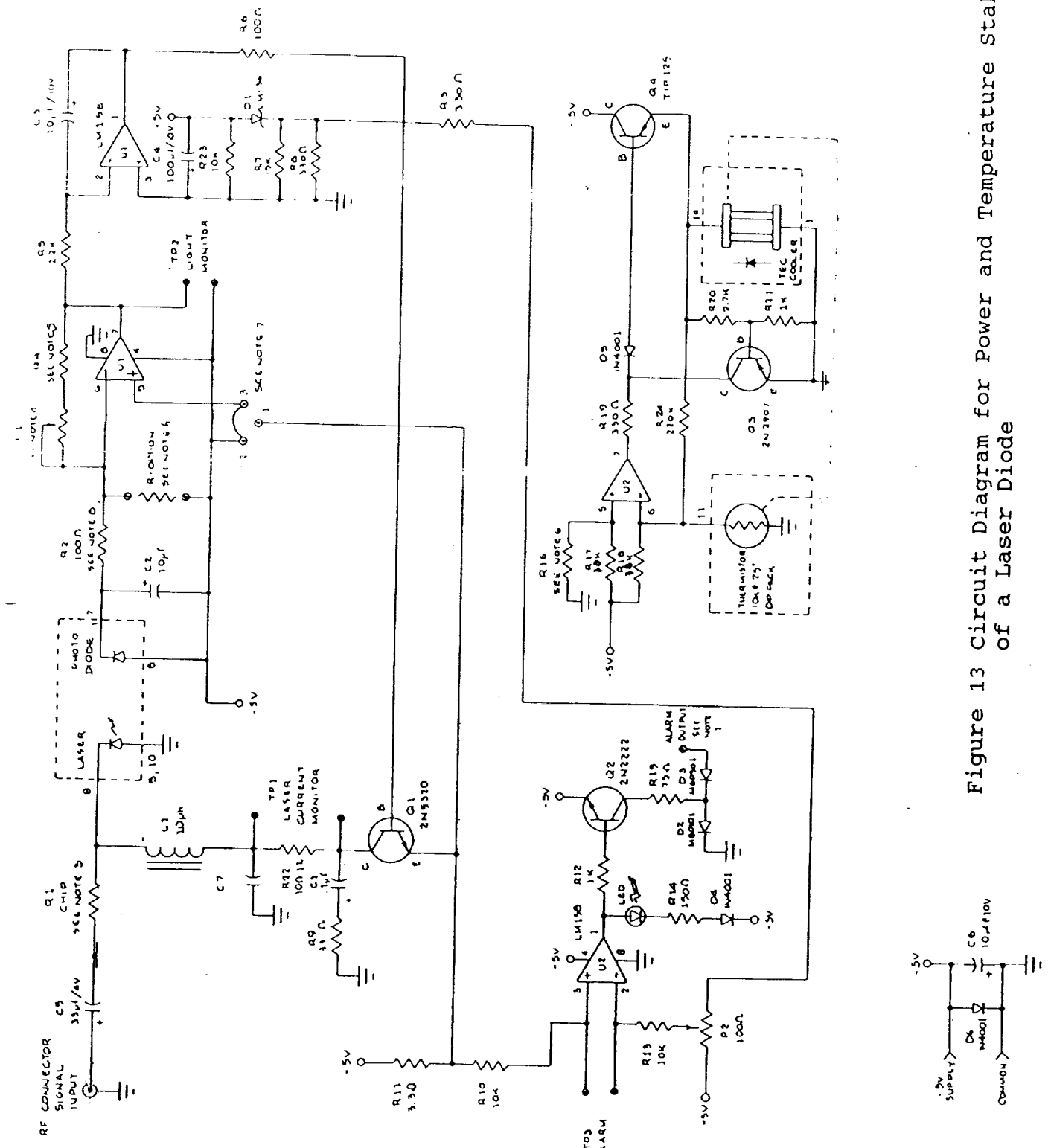


Figure 13 Circuit Diagram for Power and Temperature Stabilization of a Laser Diode

LDM-4412

Temperature Controlled Laser Diode Mount

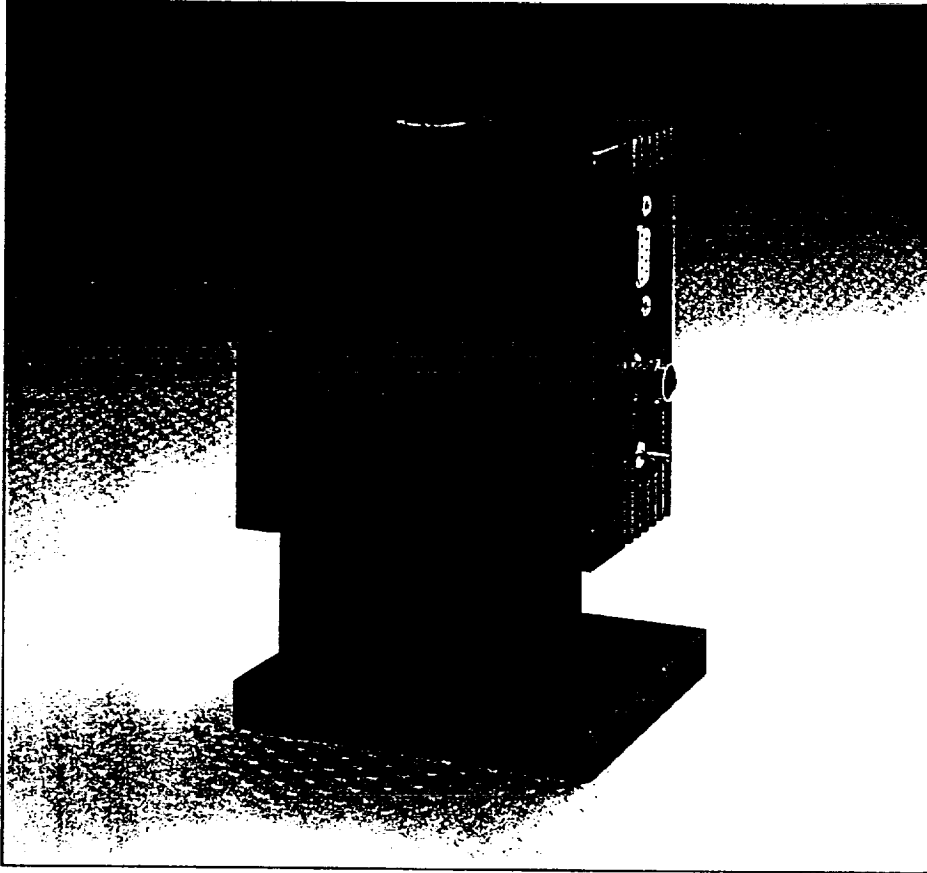


Figure 14 Housing for Two Stage Temperature Controlled Laser

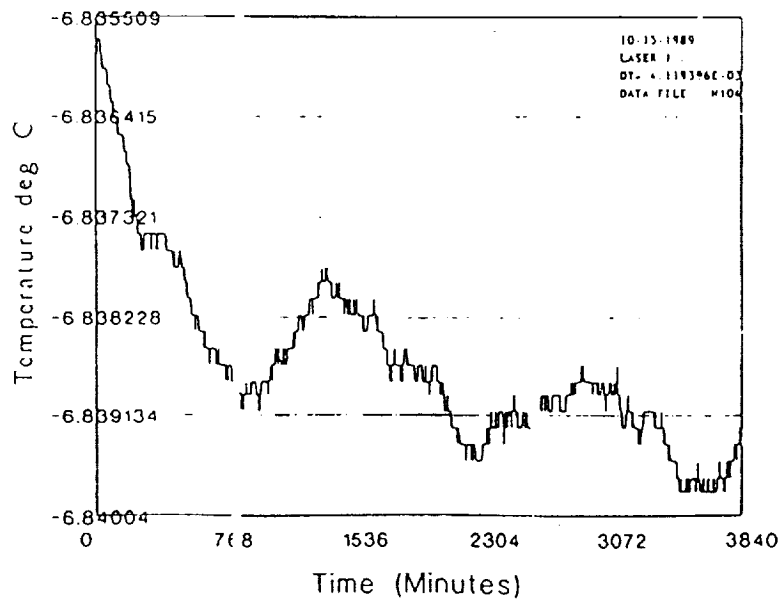
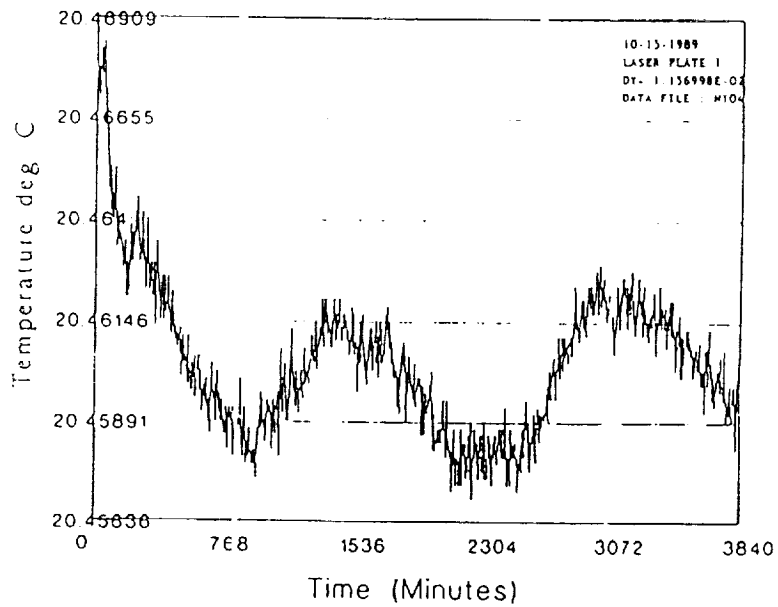
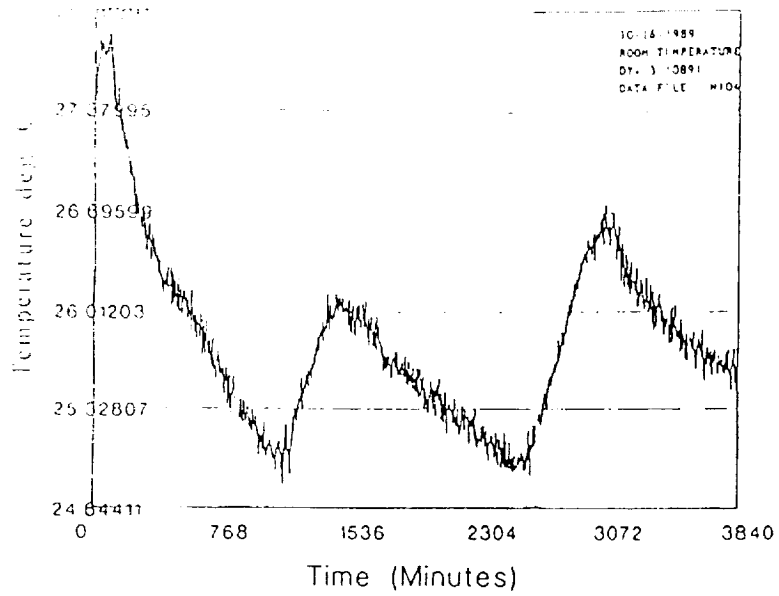
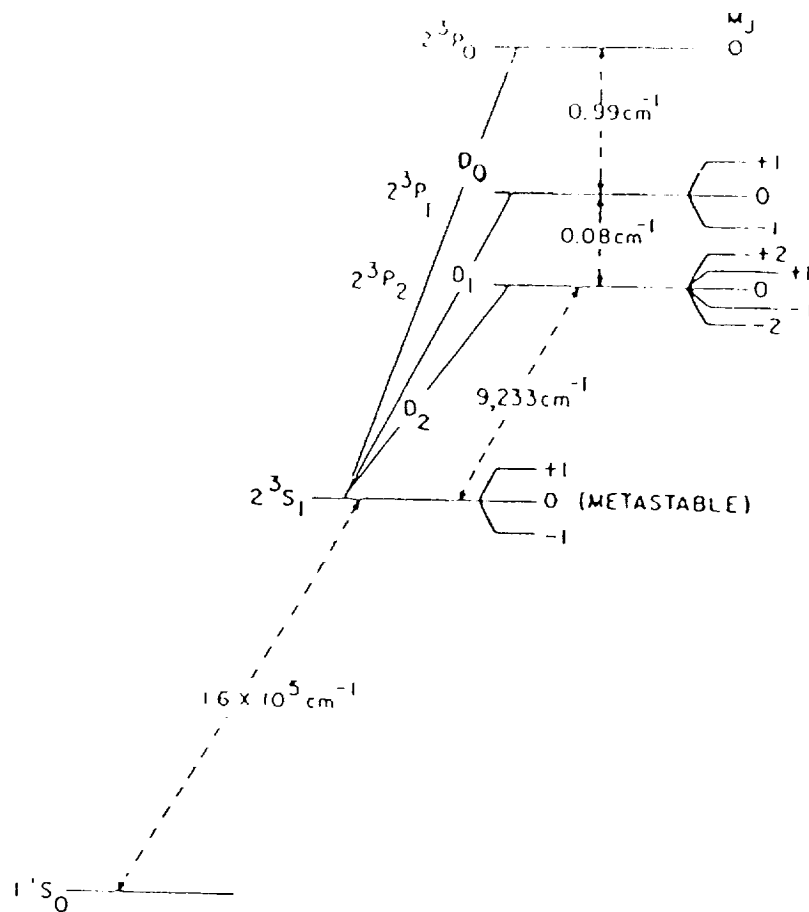


Figure 15 Temperature Stability of a Two Stage thermo-electric cooler controlled Laser Package

8. Temperature and Current Tuning of Laser Diode to He lines

The energy levels involved in optical pumping for He magnetometer is shown in Figure 16. The main absorption lines are D_0 (10829.08 Å), D_1 (10830.25 Å) and D_2 (10830.34 Å). The separation between D_0 and D_1 line is 1.17 Å, while the separation of D_1 and D_2 lines is only 0.09 Å. The Doppler width is about .05 Å, therefore, D_1 and D_2 lines can not be separated, we will call the merged lines D_{12} line. The D_{12} line is a much stronger absorption line not only because it consist of two lines, but also because each of the two lines has multiple degeneracy. The tuning of the diode laser wavelength to the He absorption lines are performed by focusing the laser output into a He cell as shown in Figure 17, which was supply by JPL. For a fixed laser drive current the temperature of the laser can be changed so that the lasing wave length will coincide with the He absorption lines. When this occurs the He cell will have strong florescence at 1.083 μm wavelength. This phenomena can be easily observed using a silicon CCD TV camera. Figure 18 shows a typical tuning characteristics of a 1083 nm laser we can obtain resonance absorption on both D_0 and D_{12} lines. We can observe florescent for temperature ranging from 13.8°C to 18.3°C and drive current from 170 mA to 260 mA. The electric power required for the laser is typically 0.4 Watts. For drive current increase of 10 mA, the temperature has to be lower by 0.33°C. To shift the wavelength from D_0 line to the longer wavelength D_{12} line the temperature has to be increased by 1.4 degrees C. Which corresponds to peak wavelength shift of .87 Å/degrees C. Figure 19 Shows the tuning

curve of another laser diode that was housed in a two stage temperature controlled package and delivered to JUL. For this laser diode the operation temperature has to lower at about 7 to 12 degrees C. It requires 1.35 degrees C temperature change to shift from D_0 line to D_{12} line. The temperature dependence of the peak wave length is about $0.9 \text{ \AA} / \text{degrees C}$.



Energy levels of helium involved in optical pumping.

D0 : 10829.08 Å (9234.395 cm⁻¹) 2.767775x10¹⁴

D1 : 10830.25 Å (9233.397 cm⁻¹) 2.767476x10¹⁴ 29.9 GHz

D2 : 10830.34 Å (9233.320 cm⁻¹) 2.767453x10¹⁴ 2.3 GHz

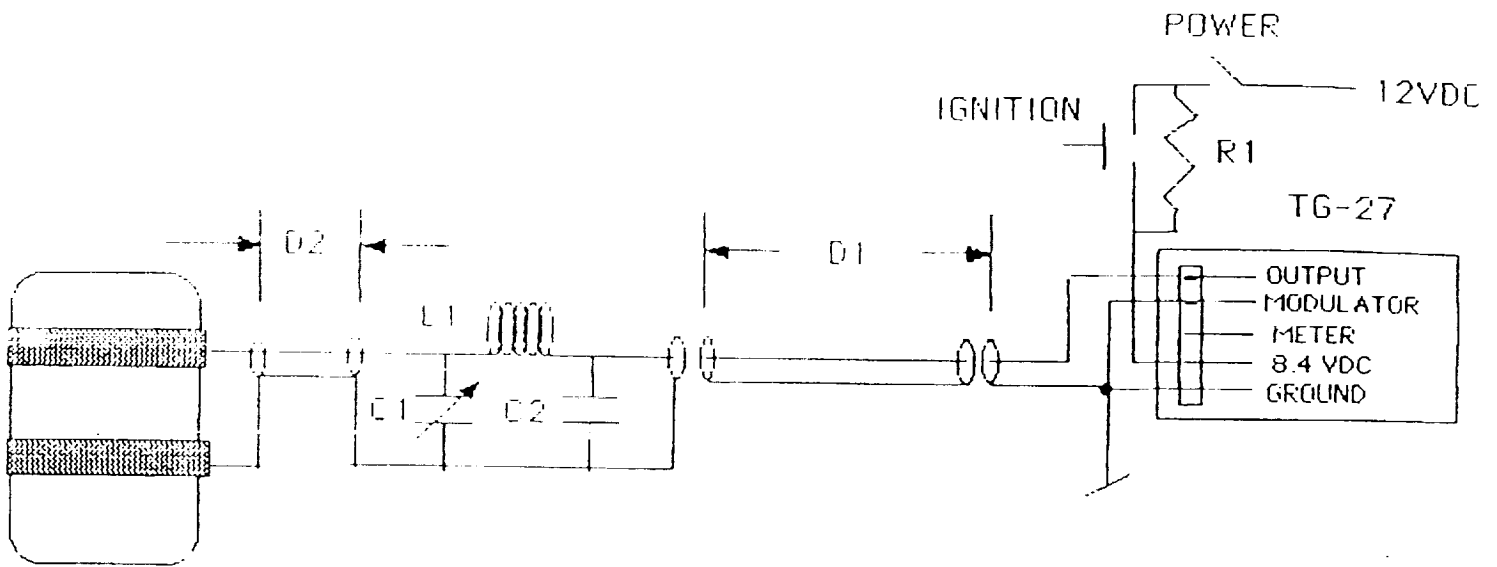
$$\text{Doppler Half-Width} = \sqrt{\frac{kT}{m}} \nu = \sqrt{\frac{1.38(-23)*300}{1.6(-19)*4*9.38(6)}} \nu = .73 \text{ GHz (300 K)}$$

$$.84 \text{ GHz (400 K)}$$

$$\text{Line Width} : \Delta \nu = \frac{c}{\lambda^2} \Delta \lambda = 25.578 \text{ GHz (1 Å) at } \lambda = 1.083 \mu\text{m}$$

$$1 \text{ GHz} \cong .039 \text{ Å}$$

Figure 16 Energy Diagrams of HeII Absorption Lines



C1 - 15pf D1 - 12" CELL PRESSURE .8 TORR
 C2 - 100pf TG 27
 L1 - 2.2uH R - 25 ohm MFG FUTABA

He Cell and RF source

JVA 1-19-90

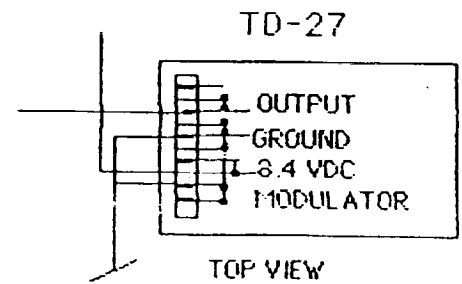
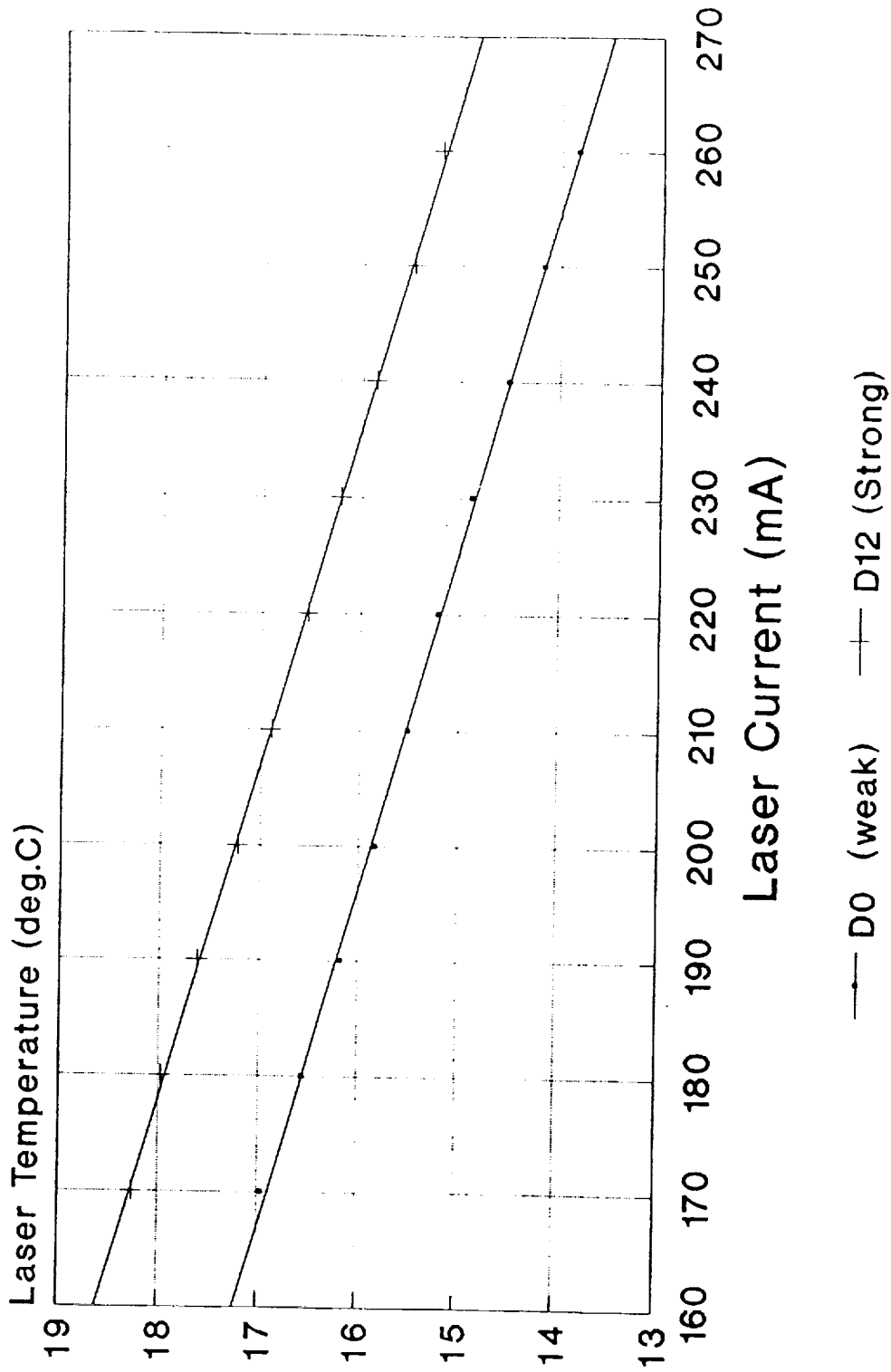


Figure 17 Diagram of He Cell and RF source

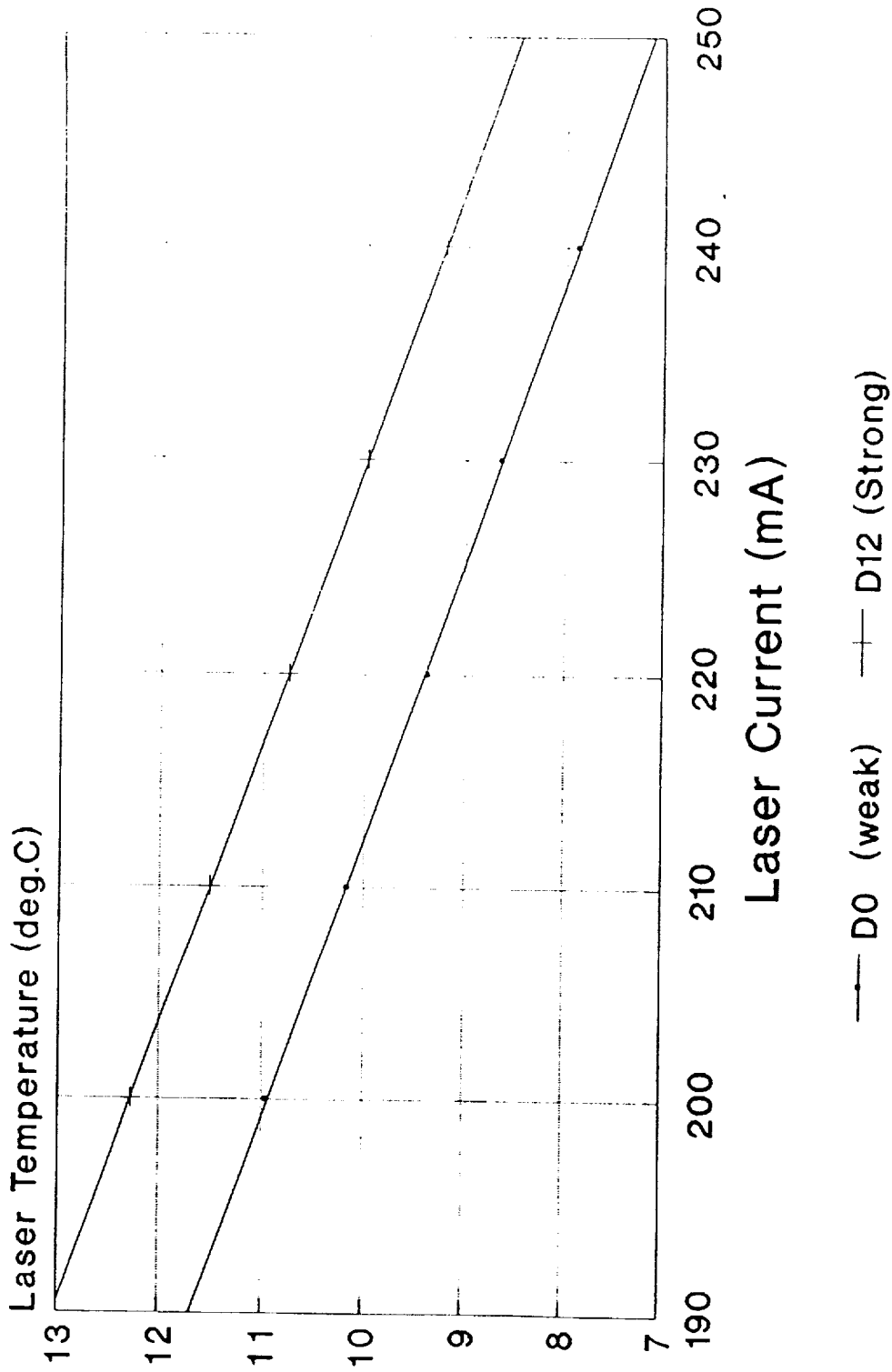
JPL-10 TUNING CHARACTERISTICS



Temp. & Current Tuning for Helium lines

Figure 18 Temperature and Current Tuning Characteristics of Laser 1.083-10 for He Absorption Lines

JPL-15 TUNING CHARACTERISTICS



Temp. & Current Tuning for Helium lines

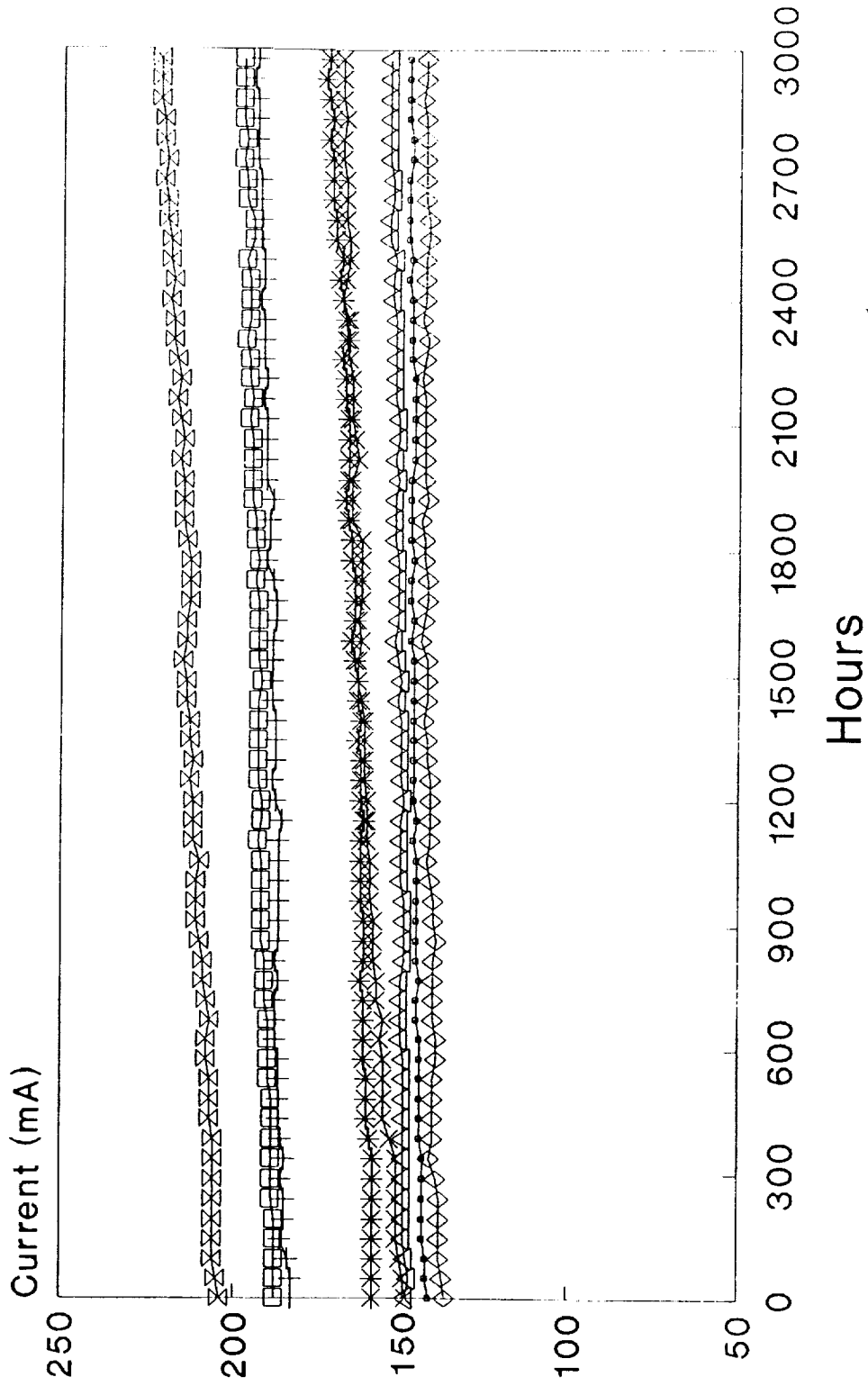
Figure 19 Temperature and Current Tuning Characteristics of Laser 1.083-15 for He Absorption Lines

9. Life-Test

Life-test of the 1.083 μm lasers have been performed using the automatic power control (ABC) mode of operation. A total of eight lasers have been life-tested at 30 degrees C for over 3000 hours. Figure 20 shows the data for life-test of the lasers. After operation of 3000 hours no laser has failed. The data shows similar trend as that of other quaternary GaInAsP/InP lasers operating at 1.3 μm or 1.55 μm wavelength region. Since the component material are the same we can expect the life time to be similar to that of 1.3 μm or 1.5 μm lasers which has been established to be over 10^6 hours (> 100 years). However, to establish a reliable life-time for the 1.083 μm laser, longer and accelerated life test should be performed.

1083 nm LASER LIFE TEST

Wafer:55 Power:5 mW Temp:30C



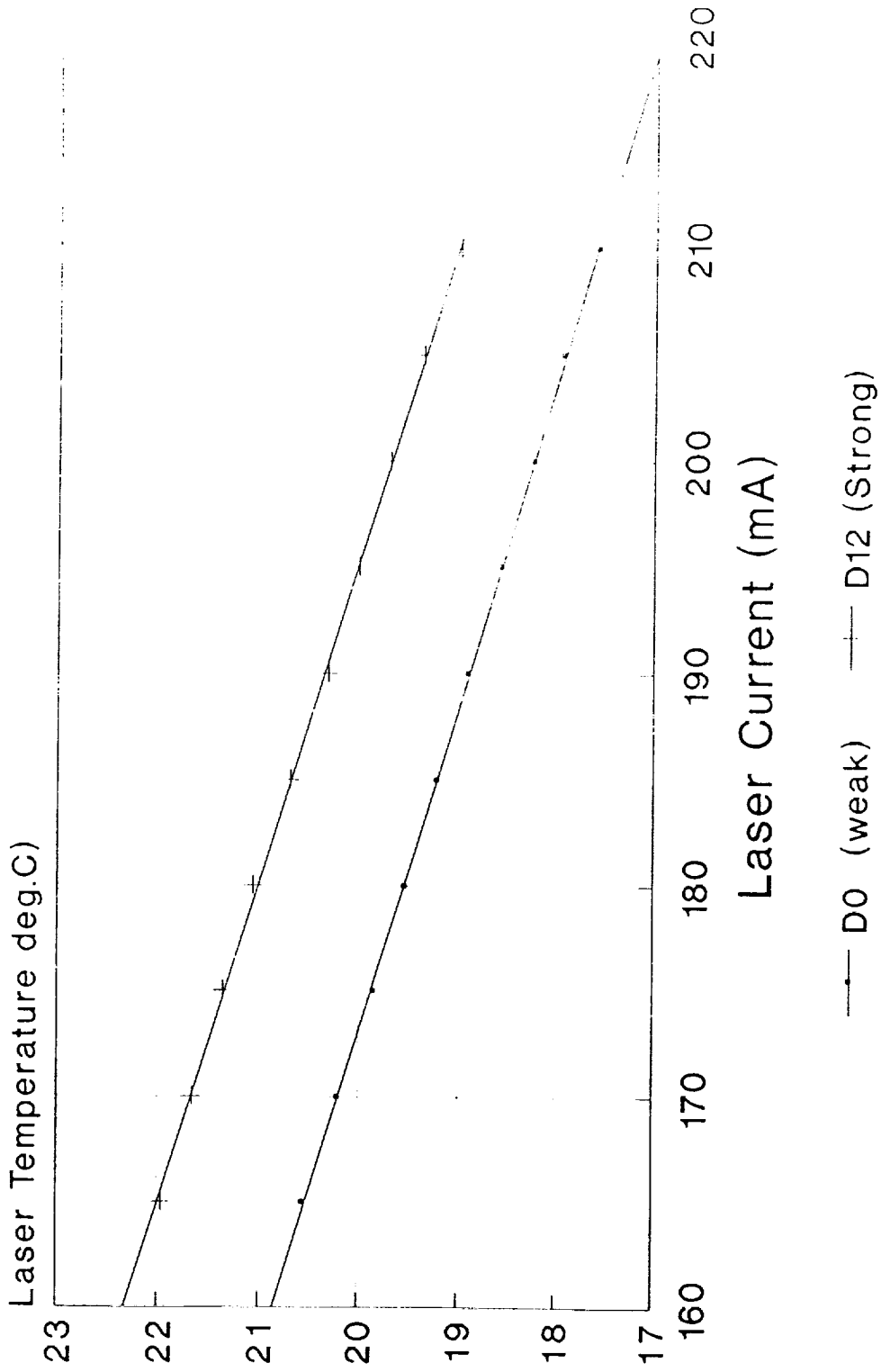
Life Test of InGaAsP/InP 1083 nm Laser

Figure 20 Life-Test Data of 1083 nm Laser Diodes

10. Delivery of Prototype Units

Two shipments of devices have been made for the contract. The first shipment were made on January 19, 1989. Which included two devices with the tuning characteristics as shown in figure 18 and figure 19. The serial number of the devices are JPL-10 and JPL-15. The later device have been housed in a two stage thermo-electric cooler temperature controlled housing as shown in figure 14. A preliminary test at JPL and Polatomics shows that the laser is very sensitive to feed back reflections, which produces unwanted noise. The second shipment included two additional devices in TO-8 packages with removable caps. Which were manufactured and shipped to JPL magnetometer Laboratory on May 1, 1991. The serial number for the two devices on second shipment are 1.083-19 and 1.083-23. Their tuning characteristics curves are shown in figure 21 and figure 22 respectively.

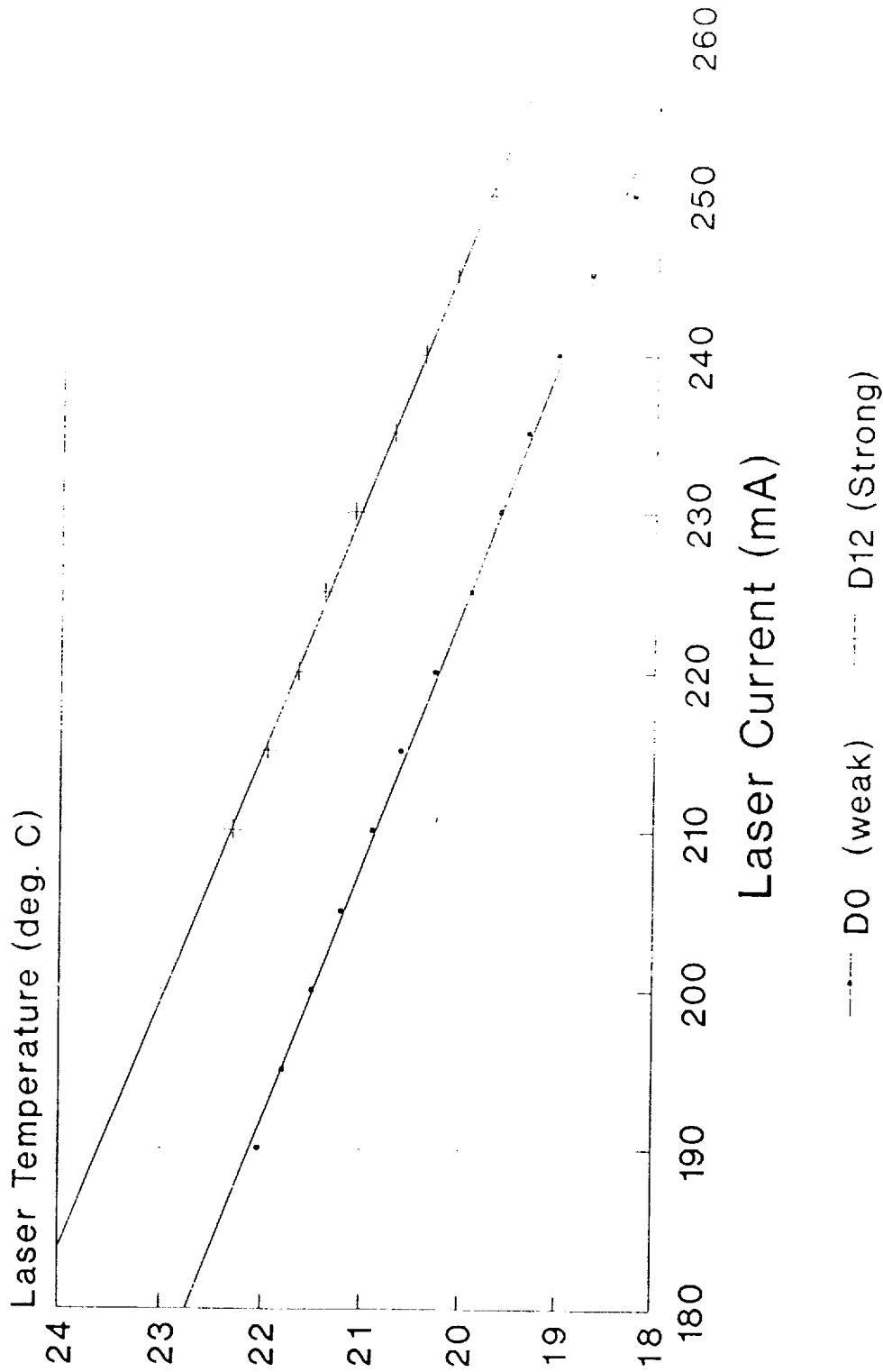
1.083-19 TUNING CHARACTERISTICS



Temp. & Current Tuning for Helium lines

Figure 21 Temperature and Current Tuning Characteristics of Laser 1.083-19 for He Absorption Lines

1.083-23 TUNING CHARACTERISTICS



Temp. & Current Tuning for Helium lines

Figure 22 Temperature and Current Tuning Characteristics of Laser 1.083-23 for He Absorption Lines

11. Conclusions

A InGaAsP/InP semiconductor laser with emission wavelength at 1.08 μm has been successfully developed by using a channelled substrate narrow stripe structure. CW operation with an output power of over 10 mW has been achieved. The lasers have a typical threshold current around 80 mA and over 10 mW output power at an operating temperature of 20 degree C. The emission wavelength is tunable with wide temperature and current ranges to match the HeII absorption lines $D_0(10829.08 \text{ \AA})$, $D_1(10830.25 \text{ \AA})$ and $D_2(10830.34 \text{ \AA})$. A temperature and power stabilization electronics circuit has also been design to control the output power and temperature of the laser to within 0.02°C. This temperature control is required for the lasing wavelength to stay within the Doppler width of the absorption lines. Temperature stability of within 0.005°C has been demonstrated over a few weeks period. Operation life-test of the lasers has also been performed at 30°C. No failure or degradation has been observed over 3000 hours of life-test. Four operating units, which can be tuned to all the absorption lines, have been delivered to JPL Magnetometer Laboratory.

The project goals as set by the NASA SBIR program have been completely and successfully accomplished.

The Project was carried out with Dr. C. S. Wang as principal investigator, and Mr. Jan-Shin Chen, Mr Ken-Gen Lu and Mr. Keng Ouyang as co-principal investigator.

12. References

- [1] E. J. Smith, B. V. Connor, and G. J. Foster, Jr., "Measuring the Magnetic Fields of Jupiter and the Outer Solar System" IEEE Trans. Magn. Mag-11, 962 (1975).
- [2] E. J. Smith, L. Davis Jr., D. J. Jones, P. J. Coleman Jr., D. S. Colburn, P. Dyal, and C. P. Sonett. " Saturn's Magnetosphere and Its Interaction With the Solar Wind" J. Geophys. Res, 85, 5655 (1980).